Finite Element Simulation using SPH Particles as Loading on Typical Light Armoured Vehicles

Geneviève Toussaint and Robert Durocher
Defence Research and Development Canada – Valcartier

Abstract

Light Armoured Vehicles (LAV) are essential to transport troops and equipment in combat and high risk zones. The emergence of non conventional threats such as Improvised Explosive Devices (IED) implies a need to reassess armoured vehicle design to improve crew survivability. To do this DRDC has been developing new experimental facilities and has conducted experimental testing to study armoured vehicle structure subjected to near field blast loadings. Numerical models of the test facility were developed to assist the design of the experimental program and to accelerate the design of improved protection systems. This paper presents results of experimental and numerical analysis, in order to compare the numerical predictions with experimental results. In this study the smoothed particle hydrodynamics (SPH) technique was applied to model the loading on the vehicle structure.

Introduction

In the actual context, the emergence of non conventional threats such as *Improvised Explosive Devices* implies a need to constantly improve the *Light Armoured Vehicles* (LAV) structure. Therefore, to assist the design of protection systems, *finite element* (FE) analysis are often used. However, one problem, which is addressed in this paper, is to use a numerical model of blast in near field that will accurately predict the structural response of the LAV. Several authors [1-2] demonstrated that the *smoothed particle hydrodynamics* (SPH) method could be used to simulate mine blast detonation under a structure. Some studies [2 to 8] have investigated the *arbitrary lagrangian eulerian* (ALE) method, as implemented in LS-DYNA®, to model blast. Although these two techniques seem promising, the SPH technique was used in this study to generate the loading on the structure and results are compared with experimental measurements.

The first and second sections of the paper describe, respectively, the experimental set-up and the corresponding FE model of a mock-up. The third section presents the result obtained using the SPH technique to simulate loading on the mock-up and provides a comparison with experimental results. Finally, conclusion and future work are presented.

Side Blast Experimental Set-up

The LAV mock-up is a testing facility developed by the Defence Research and Development Canada – Valcartier to study the reaction of LAV structure and occupants subjected to side and under belly blast attacks. The mock-up, shown in Figure 1, was designed to conduct full scale trials and assess survivability enhancement systems such as structural hull reinforcements, add-on armor systems, seating and stowage systems. The mock-up represents a 2m long section of the rear of a Canadian LAV III. It consists of rigid frames at the front and aft of the mock-up, on which a sacrificial sub-assemblies, representing the area of interest is bolted. For side blast trials, the sacrificial target is a welded assembly of the side wall, sponson top panel, sponson wall and a

section of the floor. The mock-up is equipped with wheels to provide representative geometry and masking. For this testing configuration, the total mass of the mock-up was 9600 kg.

Figure 1: DRDC Valcartier LAV III Mock-up Testing facility [9]

The mock-up was instrumented with five (5) 3-axis accelerometers mounted on the interior walls (one on at the center of the side wall, one at the center of the sponson top, one on the corner of the sponson, one at the center of the sponson wall and one at the base of the sponson wall) to monitor the local reaction of the structure. A laser displacement sensor was aimed at the corner of the sponson. Internal high speed imagery monitored the deformation of the wall and four (4) 3-axis accelerometers were mounted on the roof to measure global motion of the test rig. Wall reflected pressure measurements were taken inside the test rig. External incident pressure measurements were taken at 10 and 20 m from the charge. Figure 2 shows pictures of internal instrumentation.

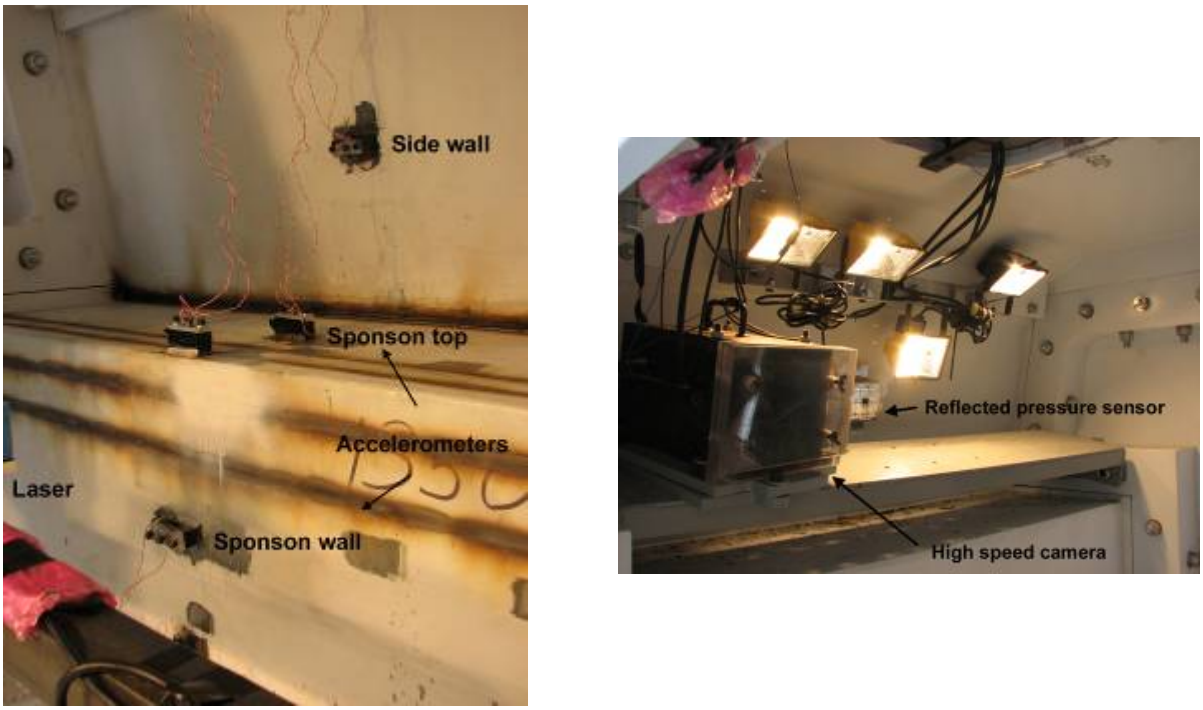

Figure 2: Internal instrumentation of the mock-up

Finite Element Model of the Mock-up

The modeling of the structure involved the creation of the geometrical model, the assignment of the materials, properties, mesh, contacts, the appropriate boundaries and the loadings. The finite element model is presented in Figure 3 and was meshed with 3826 shell elements.

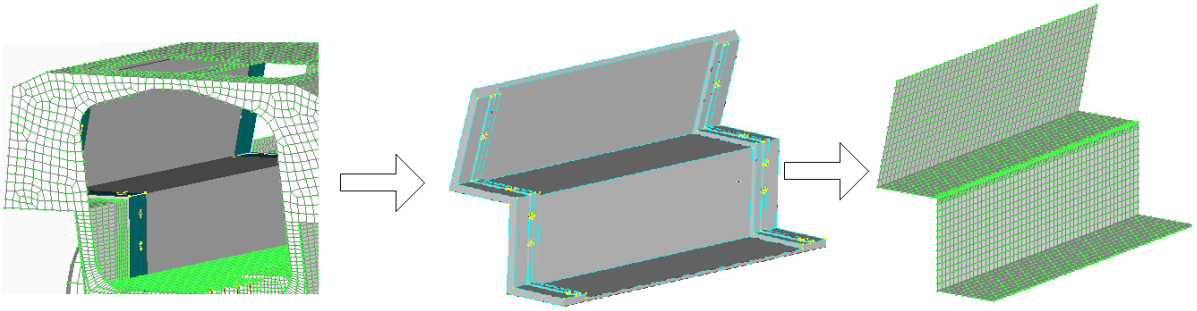

Figure 3: Finite element model of the mock-up

The steel structure was modeled using the LS-DYNA material model "*mat_kinematic_plastic*". Considering that we are only interested by the local deformation of the mock-up, for the FE modeling each side of the mock up was fixed in space as well as the top and bottom of the model. The wheels were modeled for masking purpose. The explosive parameters, like the type and quantity of explosive, the height of burst and the stand off distance, were set to match the experimental conditions. Figure 4 shows a generic representation of the numerical model used to perform the simulations.

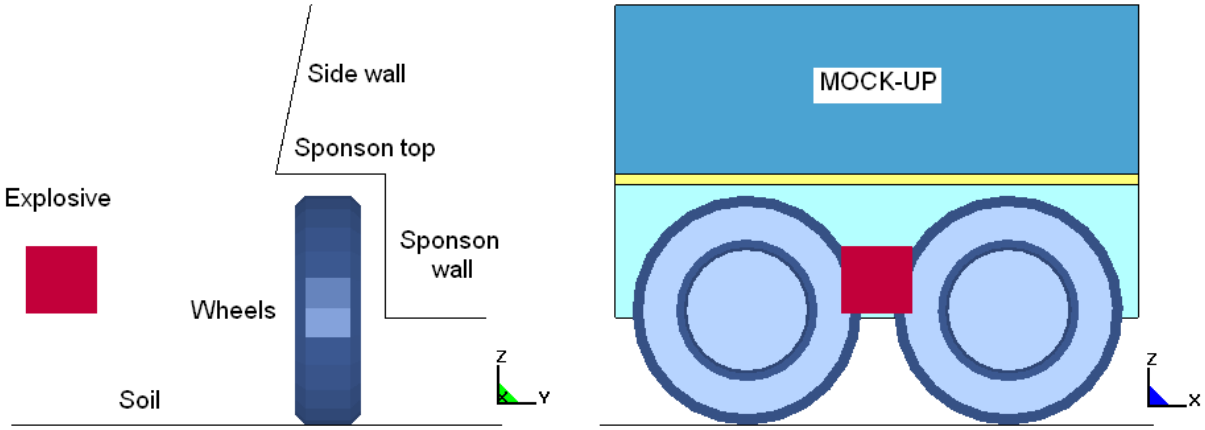

Figure 4: Numerical model of the mock-up

The properties used to model the explosive using the JWL equation of state were found in the literature [10] and are listed in Table 1 and Table 2.

Table 1: TNT Explosive properties [10]

	Explosive
Density	1630kg/m^3
Detonation velocity	6930 m/s
Chapman-Jouget pressure	21.0GPa

Table 2: JWL EOS parameters for TNT [10]

	EOS parameters
a	371.2 GPa
b	3.231 GPa
r1	4.15
r2	0.95
Omega	0.30
Internal energy density (Eo)	7.0 GPa - m^3/m^3

The explosive was modeled using different settings of SPH particle numbers. As an example, structural deformations associated with 3840 (mesh 1), 30720 (mesh 2) and 245760 (mesh 3) numbers of particles are shown in Figure 5 (for the same initial mass of explosive). It was observed from this mesh analysis that a large number of SPH particles are necessary to avoid local effect of the particles on the structure and to reproduce a hydrodynamic behavior of the loading on the structure. To limit the calculations on the particles, a box envelope was specified using the "*control_sph*" card. Also, a rigid wall condition was generated at the ground level to allow reflection of particles on the ground. Finally, two types of contact were used: "*contact_automatic_nodes"* between the SPH particles and the mock-up structure and "*contact_automatic_surface"* between all the lagrangian entities. The responses of the mock up structure to the SPH explosive loading, using 219600 particles is depicted in Figure 6.

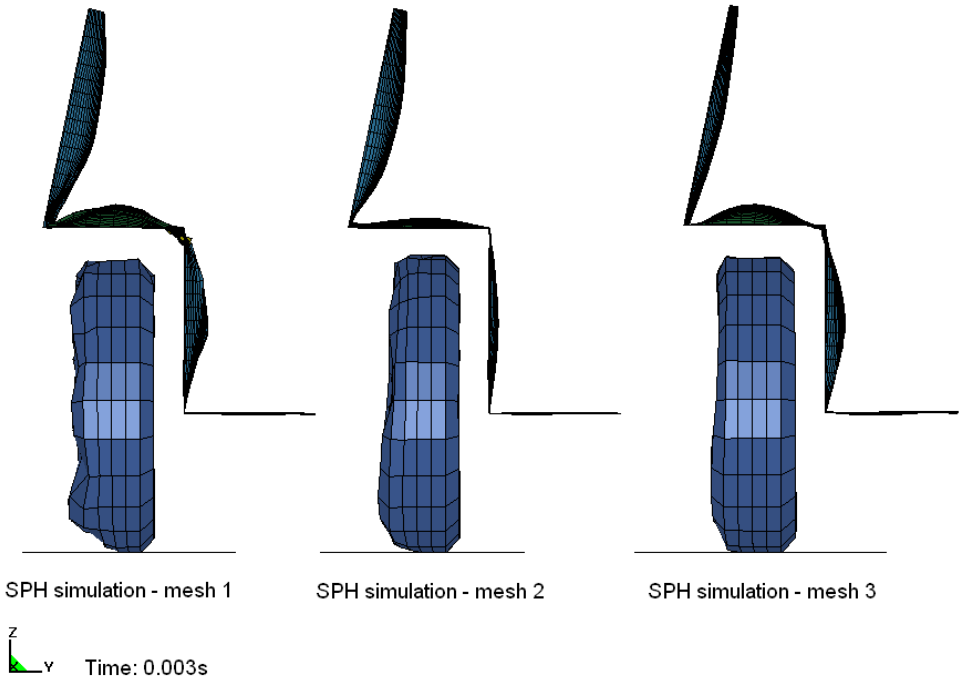

Figure 5: Influence of the SPH mesh on the structure

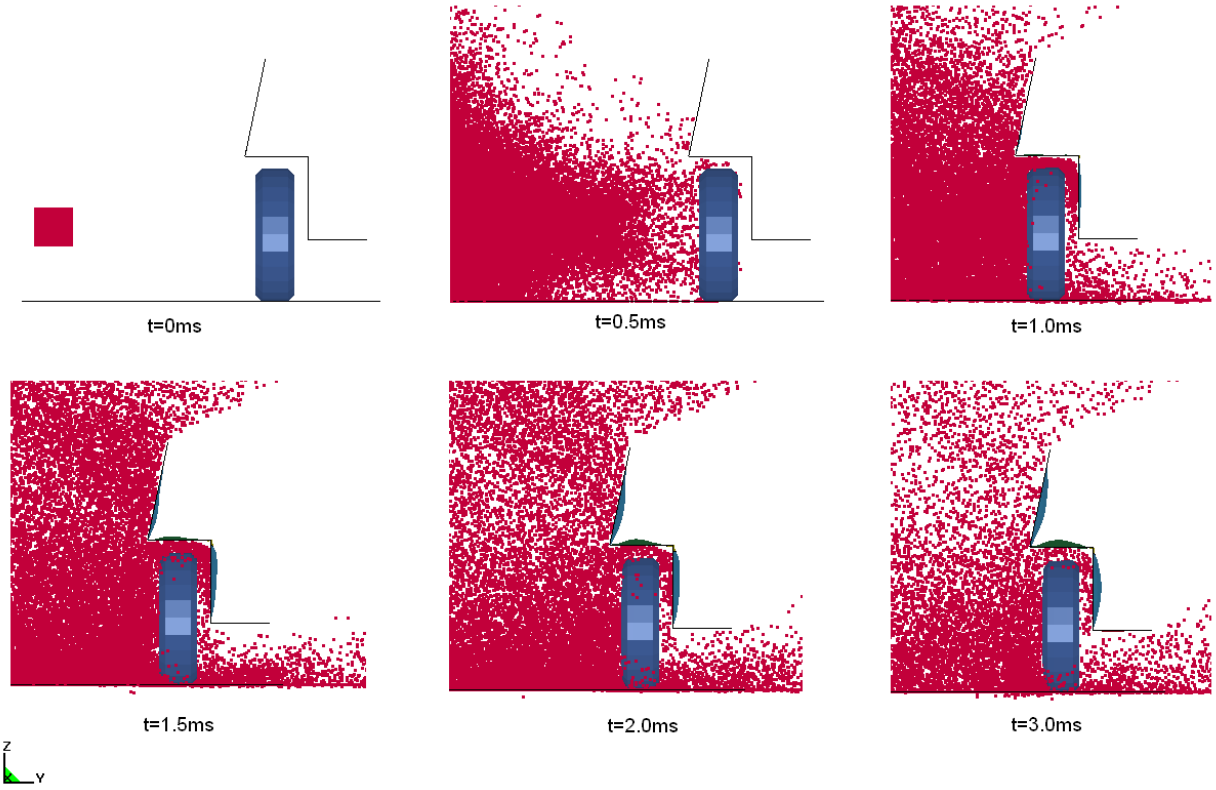

Figure 6: SPH particles impacting the mock-up structure

Numerical results were compared with experimental measurements. Experimental accelerations measurements were integrated to generate velocity history curves for the monitored points. Only the principal axis of deformation for three (3) of the monitored points are used for the comparison. Figure 7 to 9 show a comparison of the numerical simulation and experimental measurements. Reference axes are shown in Figure 5 and 6 (Y-axis positive toward the inside of the vehicle and Z-axis positive upwards). Results obtained with 219600 particles are presented in relative ratio of the numerical simulation versus experimental results, i.e. the experimental and numerical velocities plotted in Figure 7 to 9 were divided by the highest experimental velocity obtained for their respective component Vy - side wall, Vz - sponson top and Vy - sponson wall.

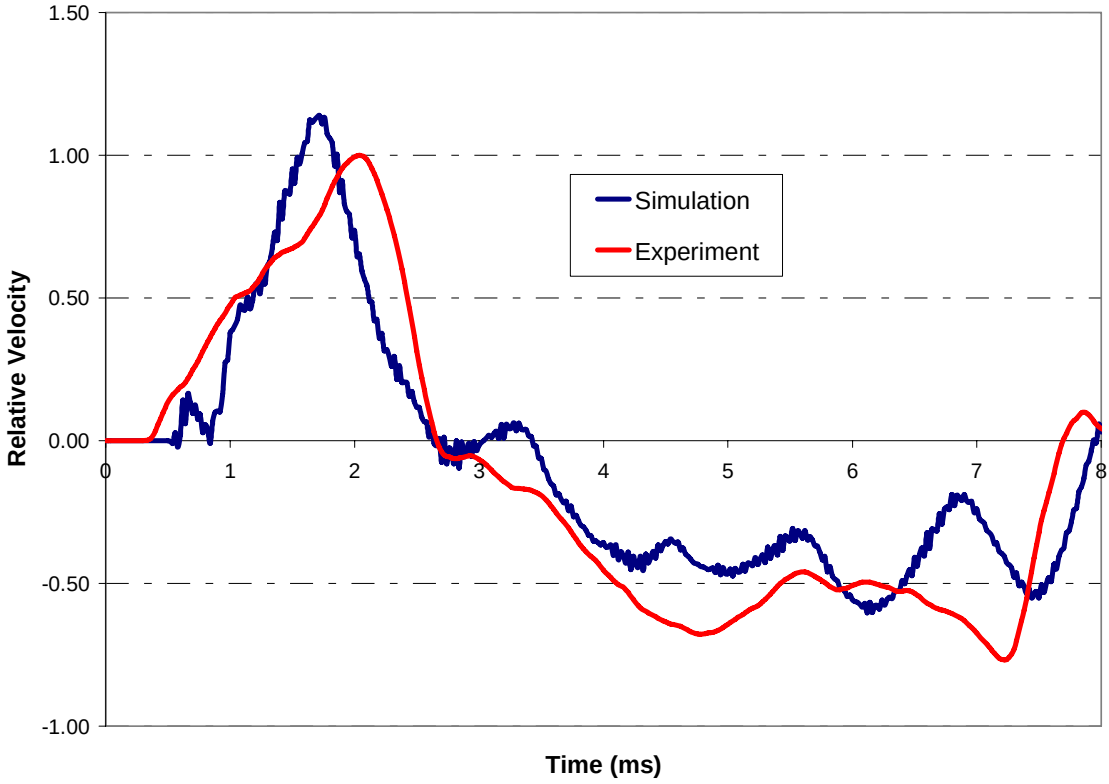

Figure 7: Comparison of the relative velocities "Vy" of the side wall

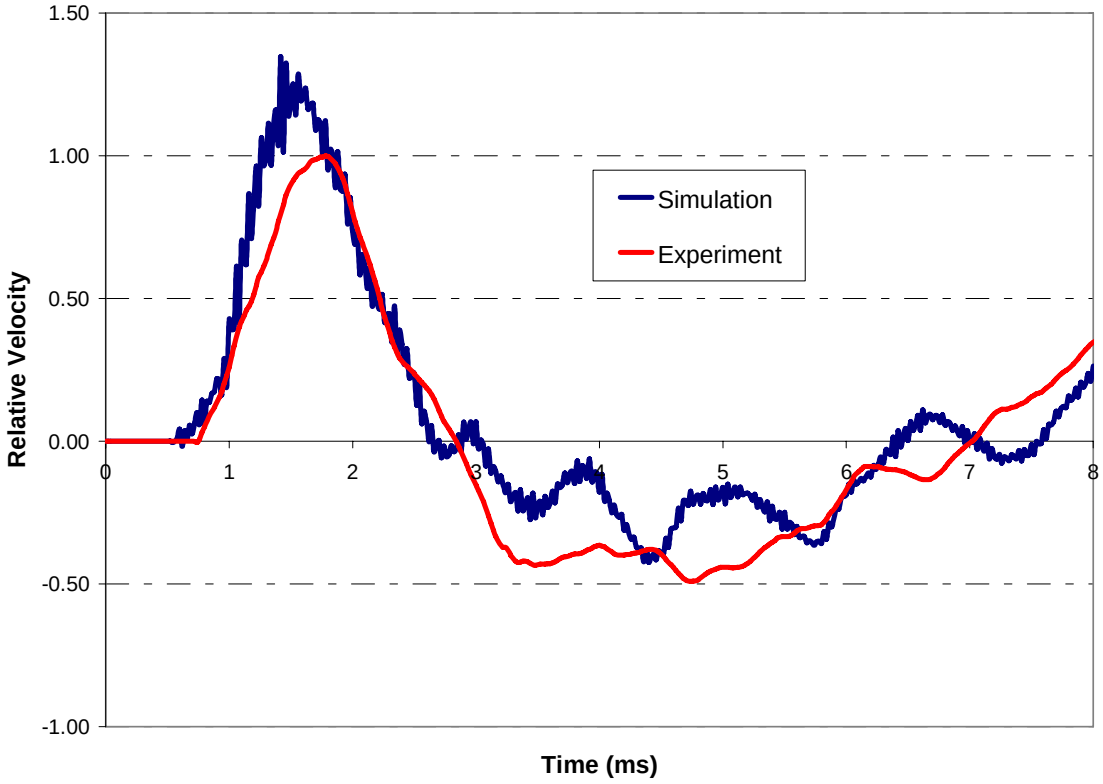

Figure 8: Comparison of the relative velocities "Vz" of the sponson top

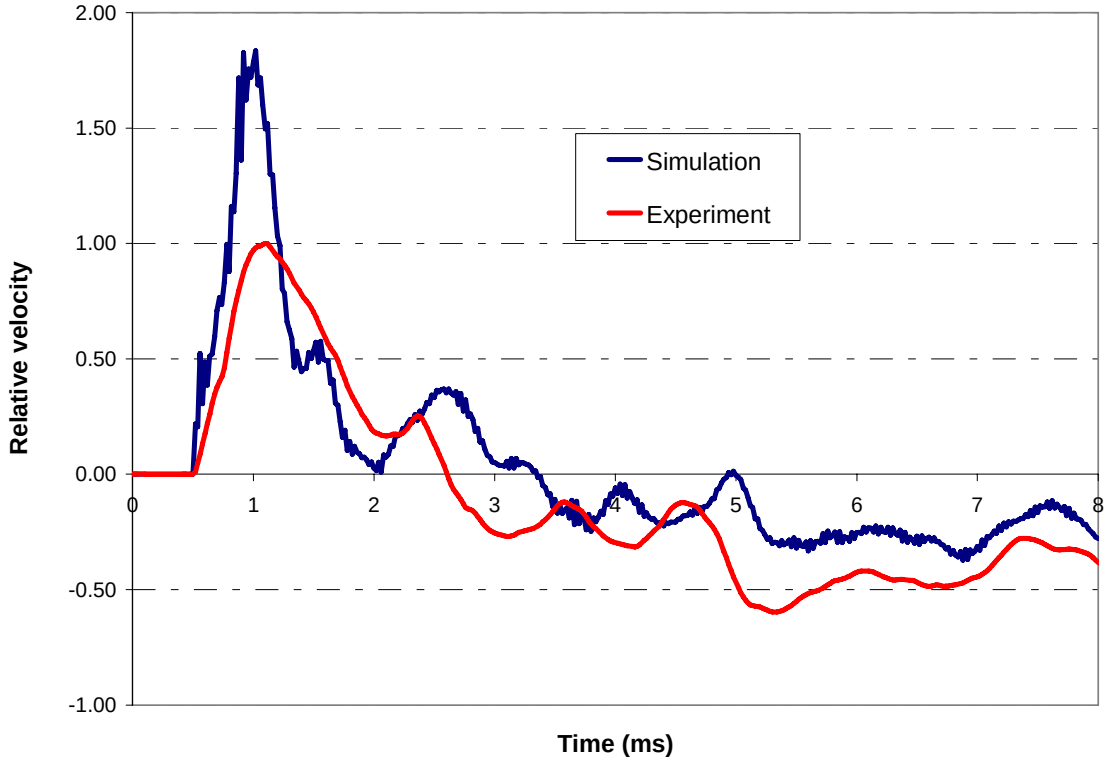

Figure 9: Comparison of the relative velocities "Vy" of the sponson wall

As shown in Figure 7 and Figure 8, a very good correlation is observed between the horizontal deformation velocity of the side wall and the experiment and between the vertical deformation velocity of the sponson top and the experiment. However, in Figure 9 the horizontal deformation velocity of the sponson wall is approximately 75% higher than the experimental values. Such results could be explained by the influence of several factors like: the type of material model, the parameters used for the materials and JWL EOS, and the mesh of the structure. Also, a conversion factor was applied to the explosive mass used in the experiment to correspond to an equivalent TNT mass. As well, the initial geometry chosen for the explosive could influence the results and should be studied. Moreover, in the experiment the complete mock-up weighed 10 tons and was free to move where as in the numerical model, the outside boundaries of the mock-up were fixed and did not allow any global motion of the structure. Finally, only one set of experimental data were generated so far. Additional tests, under the same conditions would be required to assess the normal experimental variation. All the factors mentioned above should be further studied to refine the loading using SPH particles and in order to validate it, this model of loading should be used with other initial conditions and apply to different vehicle structures and should be compared to experiments. Although there were many factors that could influence the response, overall the numerical results matched well the experiment.

Conclusion

This paper presented results obtained using the SPH technique to simulate loading on representative LAV structure and provided comparison with experimental data. The presented model over predicted the peak velocity of the sponson wall, but showed very good correlation with experimental result for the side wall and sponson top. For all compared points, the time response of the structure was well captured by the numerical analyses. The current model has shown it can be used to predict structural response of the mock-up structure and can be used to compare protection system options for the given initial conditions. However, to be able to use this SPH loading for other scenarios, numerical analyses will be performed with other initial conditions and apply to different vehicle structures. Further work is required to generate additional experimental data and assess numerical model parameters in order to improve the model accuracy.

Future Work

During the analyses, many numerical problems were addressed (parameters, mesh, contact, etc.) but still, several considerations need to be further explored. Furthermore, to eventually assess both methods, SPH and ALE, and identify which one to use in given applications, the ALE technique will be investigated.

References

1. Lacome J.-L., *Analysis of Mine Detonation, SPH analysis of structural response to anti-vehicles mine detonations*, LSTC, 2007.
2. http://www.ara.com/offices/Blast_Response.htm
3. Hilding D., *Simulation of a detonation chamber test case*, 3rd European LS-DYNA Users Conference, 2001.
4. Vulitsky M. Z. and Karni Z. H., *Ship Structures subject to high explosive detonation*, 7th International LS-DYNA Users Conference, 2002.
5. Mullin M. J. and O'Toole B. J., *Simulation of energy absorbing materials in blast loaded structures*, 8th International LS-DYNA Users Conference, 2004.
6. Cendón D. A., Gálvez F., Enfedaque A. and Sánchez-Gálvez V., *Analysis of armoured vehicles blast protection by using finite element codes*, 23rd International Symposium on Ballistics, 2007.
7. Li W.-C., Yu W.-F. and Cheng D.-S., *Increasing initial internal energy of air elements near explosive for fluid-structure models of a steel plate subjected to non-contact explosion*, 6th European LS-DYNA Users Conference, 2007.
8. Larsen M. B. and Jorgensen K. C., *Landmine protection of armoured personnel carrier M113*, 6th European LS-DYNA Users' Conference, 2007.
9. Weapons Effects and Protection Section, Defence Research and Development Canada – Valcartier, 2008.
10. Dobratz B.M. and Crawford P.C., *Properties of Chemical Explosives and Explosive Simulants*, UCRL-52997 Change 2, Lawrence Livermore National Laboratory, 1985.
11. LS-DYNA Keyword User's Manual Version 971, Livermore Software Technology Corporation, Livermore, 2007.
12. www.dynaexamples.com
13. www.dynasupport.com
14. www.lsdyna-portal.com/index.3.0.html